THE JOURNAL OF PHYSICAL CHEMISTRY A

pubs.acs.org/JPCA Article

Determinant Factor for Thermodynamic Stability of Sulfuric Acid–Amine Complexes

Jia Han, Lei Wang, Hanhui Zhang, Quyan Su, Xiaoguo Zhou,* and Shilin Liu*

Cite This: J. Phys. Chem. A 2020, 124, 10246–10257 Read Online

ABSTRACT: Atmospheric amines are thought to play significant roles in the nucleation of sulfuric acid-mediated aerosol particles. Their enhancing effects on the stabilization of the related complexes have formerly been correlated with the amine base strength, but there are a few exceptions reported. In this work, the influence of seven alkylamines on the thermodynamic stability of sulfuric acid–amine complexes has been theoretically investigated, e.g., ethylamine, propylamine, isopropylamine, *tert*-butylamine, dimethylamine, ethylmethylamine, and trimethylamine. For all primary and secondary amine-mediated complexes, a dual hydrogen bond configuration is generally suggested in the most stable isomer. The stabilization of this special structure predicted by the electrostatic potential distribution on the molecular surface of amines exactly agrees with the base strength sequence, providing crucial evidence for the previous deduction of correlation between the base strength and the enhancing effect. Meanwhile, the considerable van der Waals interactions are found between the free hydroxyl of sulfuric acid and the β-methyl group of amine, resulting in the extra stability for sulfuric acid–dimethylamine and sulfuric acid–ethylmethylamine complexes. Therefore, the electrostatic potential distribution of amines is the essential determinant factor for the thermodynamic stability of the relevant complexes. Our conclusions provide new insight into a way to evaluate the enhancing abilities of amines in aerosol particle nucleation.

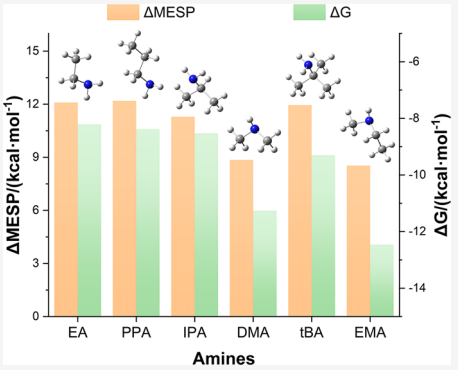

1. INTRODUCTION

Aerosol particles in the atmosphere have attracted extensive attention because of their crucial impact on many environmental-related issues, e.g., climate change, air quality particularly in urban areas, and public health.[1−6] It is well-known that nucleation in the gas phase is the initial step during the formation of atmospheric aerosol particles.[7−11] Although a number of efforts have been made to study the nucleation processes, several unknown facts at the molecular level still remain, especially concerning the promotion mechanisms by other chemicals and the cluster compositions of freshly nucleated particles.[1,9,12]

As the most common nucleation species for atmospheric aerosols, sulfuric acid dominantly contributes to the formation of critical nucleus.[13−15] In the gas phase, sulfuric acid is mainly derived from the reaction of sulfur oxide and OH radicals produced by the UV photolysis of water vapor.[16,17] Then, it can be easily converted into the condense phase in the presence of water because of its strong hygroscopicity.[18,19] However, it is unexpected but true that the binary homogeneous nucleation of sulfuric acid and water is difficult to be observed unless both substances are supersaturated in vapor.[17,20−22] Thus, a number of other molecules with low volatility, such as ammonia, amines, and iodide molecules, have been suggested to be involved in the related particle formation.[15,20,22−34]

As the ternary inorganic reaction of sulfuric acid, water, and ammonia was confirmed to be responsible for aerosol nucleation under extremely cold conditions of the middle and upper troposphere,[35,36] ammonia was proposed to play an important reactant role in stabilizing small sulfuric acid-water clusters by forming ammonium sulfate and bisulfate salts.[22−24,35,37] However, this inorganic reaction mechanism was unable to explain the unexpectedly fast formation rate and high concentration of sulfuric acid-containing aerosol particles in the atmosphere yet. Therefore, nucleation and subsequent growth of newly formed particles should be contributed by other chemicals, especially in the highly polluted urban atmosphere.[22,27,38,39] The corresponding acid–base reactions might predominantly contribute to atmospheric aerosol formation and their growth.[40−43]

Amines are the common organic derivatives of ammonia and can be released from wide sources.[44] Although their concentrations in atmosphere are usually lower than ammonia,

Received: August 30, 2020
Revised: November 14, 2020
Published: November 25, 2020

https://dx.doi.org/10.1021/acs.jpca.0c07908
J. Phys. Chem. A 2020, 124, 10246−10257

amines have stronger alkaline and faster reaction rates with sulfuric acid.[9,27,44,45] Thus, amines are the more likely organic stabilizers for the formation of sulfuric acid-containing complexes. In the competition between ammonia and amines, Murphy et al.[46] observed the formation of alkylammonium nitrate salts indeed in the presence of nitric acid. A rapid and complete conversion from ammonium salts to aminium salts was verified by Bzdek et al.[47] in small bisulfate and nitrate clusters. Apparently, the base-exchange phenomena strongly implied that aminium salts play a crucial role in salt nuclei although ammonium salts might be initially formed. The later experimental and theoretical studies also demonstrated that amines are more effective than ammonia in promoting sulfuric acid-mediated cluster nucleation.[48−50]

Following this viewpoint, Angelino et al.[40] conducted a joint study of smog chamber experiments and field measurements, and concluded that amine chemistry "may play a significant role in regions with high amine concentrations". Thus, to find the essential correlation between the physicochemical properties of amines and their enhancing effects becomes an attractive topic. Kurtén et al.[48] calculated the stabilization energies of sulfuric acid−amine complexes and correlated this stabilizing capacity with the number and size of alkyl substituents. By comparing five atmospherically relevant amines, Yu et al.[41] concluded that the enhancing effect of amine on particle formations and growth strongly depended on its basicity. Similar conclusions were obtained by Glasoe et al.[50] and Myllys et al.[51] Accordingly, it is widely accepted that amines are key stabilizers for sulfuric acid-containing clusters,[27,40,52−58] and the corresponding complex stability and particle formation rate were determined by the base strength of amines. However, Jen et al.[58] found in experiments that the stabilizing ability of methylamine on the formation of sulfuric acid−amine dimers was weaker than that of trimethylamine (TMA) and dimethylamine (DMA), while the enhancing abilities of the latter two were close, which was slightly opposite to the fact that TMA is the strongest base in the gas phase. Moreover, the base strength of amine in atmospheric particle formation cannot be simply represented by its pK_b value, gas-phase basicity, or proton affinity, which were commonly used in previous literature.[41,51] Thus, some subordinate and unknown factors might be masked beneath the base strength in the gas phase to veritably affect the thermodynamic stability of sulfuric acid−amine complexes.

In this work, the enhancing effect of amine on sulfuric acid−amine complexes has been investigated using quantum chemical calculations. Here, we have selected seven representative aliphatic amines, i.e., ethylamine (EA), propylamine (PPA), isopropylamine (IPA), and *tert*-butylamine (tBA) as primary amines, DMA and ethylmethylamine (EMA) as secondary amines, and a tertiary amine, TMA. The proton affinities and the gas-phase alkalinities of amines[59] are listed in Table S1 of the Supporting Information. The structures and energies of sulfuric acid−amine complexes have been calculated individually followed by the comprehensive thermodynamic analyses of electrostatic potential and intramolecular interaction. As a result, the dominant determinant factors for thermodynamic stability of these complexes are unveiled.

2. COMPUTATIONAL DETAILS

Since many isomers of the sulfuric acid−amine complex might be formed according to different hydrogen bond interactions, a great number of initial sulfuric acid−amine complex geometries were generated randomly by Genmer.[60] Then, every initial structure was optimized to a local minimum with the semiempirical method, PM6-DH+, with corrections for dispersion and hydrogen-bonding, using the MOPAC2016 program.[61,62] The optimized isomers were sorted in energy, and the 50 lowest-lying ones were treated with the B97-3c generalized gradient approximation functional, using the ORCA program package.[63−65] After the energy correction, these low-lying isomers with an energy gap of less than 10 kcal·mol^{-1} were reoptimized using the hybrid B3LYP-D3(BJ) functional with the 6−311++(3df,3pd) basis set, using the Gaussian 16 software package.[66,67] Then, the global minimum was identified finally for each sulfuric acid−amine complex. Actually, the credible performance of the functional B3LYP-D3(BJ) level on hydrogen bonding complexes was confirmed previously.[68] Using these global minimum geometries, frequency analysis were conducted at the same level to ensure no imaginary frequencies and calculate zero-point energy corrections. Single point energy calculations were performed using the highly accurate CCSD(T)/def2-TZVP level of theory.[69−71]

Moreover, to further verify that the optimized structures at the functional B3LYP-D3(BJ) level are global minima indeed, another two functional methods, M06-2X-D3 and ωB97XD, with the same basis set, 6−311++(3df,3pd), were applied to optimize geometries and calculate relative energies. The lowest-lying structures at the M06-2X-D3 and ωB97XD levels were approximately identical to these B3LYP-D3(BJ) results, and only a few ignorable deviations of bond lengths and angles were found. The comparison of structures and energies for these isomers are presented in detail in the Supporting Information.

Based on the optimized geometries of complexes, topology analyses were conducted using the quantum theory of atoms in molecules (QTAIM)[72−76] to interpret the bonding characteristics between sulfuric acid and amines. Noncovalent interaction (NCI) analyses were performed using the Multiwfn package.[77,78] Moreover, molecular electrostatic potentials (MESP)[79−81] were analyzed using Multiwfn software as well to study the chemical properties of each amine.

3. RESULTS AND DISCUSSION

3.1. Electrostatic Potential Analyses of Amines.

Hydrogen atoms of both N−H and C−H bonds can be attracted by oxygen atoms of sulfuric acid, while another hydrogen bonding interaction may also exist between the hydroxyl hydrogen and nitrogen atom of amine. Thus, lots of sulfuric acid−amine complex isomers can be formed according to different hydrogen bonding interactions, when sulfuric acid collides with amines. Although we randomly prepared a great number of initial complex geometries, it is practical to evaluate MESP for predicting accurate hydrogen bonding sites and analyzing intermolecular interactions, in view of the well-established significance of MESP in hydrogen bonding interaction.[79−81] The hydrogen atoms with strongly positive charge, such as those in hydroxyl and amine groups, can play the role of a hydrogen bonding donor, whereas the electron-rich atoms or the functional groups with strongly negative charge, e.g., azine, amine, and lone pair electrons of hydroxyl, usually are the hydrogen bonding acceptors. Therefore, an electrostatic potential analysis can provide useful information on hydrogen bonding interactions.

https://dx.doi.org/10.1021/acs.jpca.0c07908
J. Phys. Chem. A 2020, 124, 10246−10257

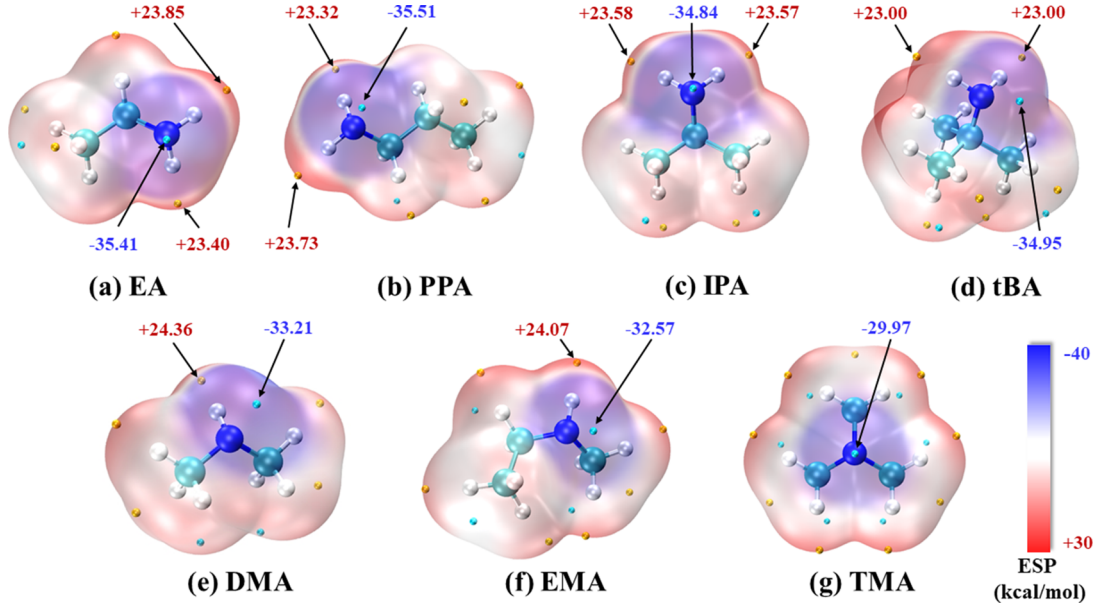

Figure 1. Electrostatic potential of amines on the 0.001 au (electrons/bohr3) molecular surface, calculated at the B3LYP-D3(BJ)/6−311++(3df,3pd) level of theory. Color coding for atoms: cyan = carbon, blue = nitrogen, and white = hydrogen.

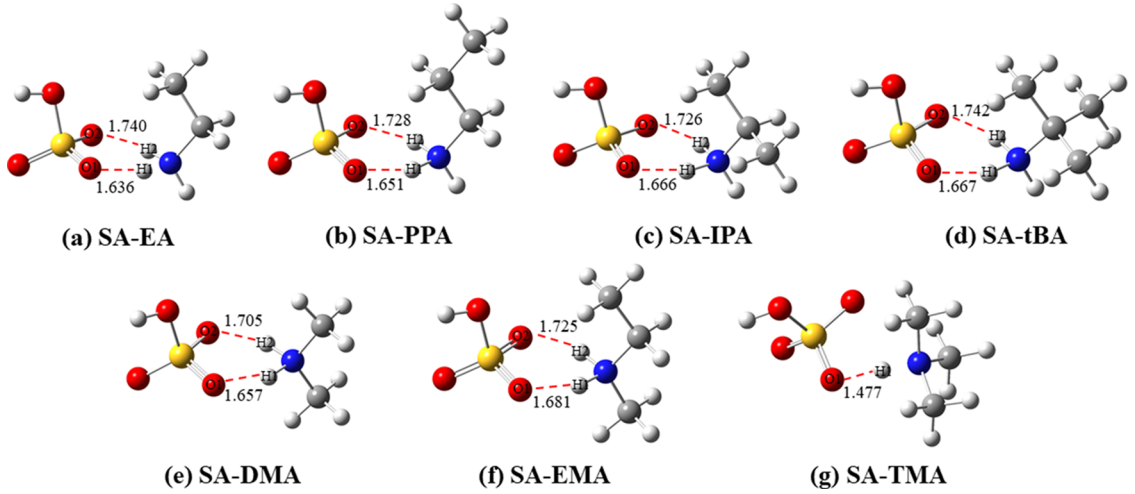

Figure 2. Optimized geometries of global minima for sulfuric acid−amine complexes, calculated at the B3LYP-D3(BJ)/6−311++(3df,3pd) level of theory. Hydrogen bond lengths are noted in the unit of Å.

Figure 1 shows the calculated electrostatic potential surfaces of seven amines, where the maximal and minimal potential values are noted and located with small yellow and cyan spheres, respectively. Although there are several local minimal and maximal points at the 0.001 a.u. isosurface of electron density, only those of higher than 10 kcal·mol^{-1} are labeled. Apparently, the minimums of MESP for all amines are located on the nitrogen lone pair electrons of the amino group. Such substantial negative potentials of ca. 30 kcal·mol^{-1} prefer to induce the occurrence of proton transfer from hydroxyl of sulfuric acid to the amino group when they meet each other. As the result, a hydrogen bond structure of S−O...H−N is formed for sulfuric acid−amine complexes. Moreover, as shown in Figure 1, the hydrogen atoms of the amino group show relatively large positive potentials (ca. 25 kcal·mol^{-1}), except for TMA, implying that the oxygen atom of sulfuric acid might probably interact with these hydrogen atoms as well. Accordingly, for primary and secondary amines containing electron deficient regions on amine hydrogen, the dual hydrogen bond configuration is the most favorable in view of electrostatic potentials. However, only a single hydrogen bond structure can be expected for tertiary amine because of the lack of hydrogen atoms in amino group.

3.2. Optimized Structures and Energetics of Sulfuric Acid−Amine Complexes. Based on the above analyses, the most stable isomers of each sulfuric acid−amine complexes were optimized and are presented in Figure 2, where the major hydrogen bond lengths were noted. The geometries and energetics of other isomers for SA-EA as a representative are summarized in the Supporting Information. For SA-EA, SA-DMA, and SA-TMA, our results are in good agreement with the previous studies,[48,53] irrespective of geometries and energetics. In general, the dual hydrogen bond configuration was verified for both primary and secondary amine−sulfuric acid complexes, while SA-TMA has the single hydrogen bond

https://dx.doi.org/10.1021/acs.jpca.0c07908
J. Phys. Chem. A 2020, 124, 10246−10257

structure, as we expected according to the electrostatic potential analyses.

For each primary amine−sulfuric acid complex, an optimized six-member ring of the dual hydrogen bond structure is shown in Figure 2a−d. Take SA-EA for instance, the breaking of one O−H bond of sulfuric acid (1.637 Å), as well as the formation of the N−H bond (1.062 Å), is accompanied by proton transfer from the acid to the amine, resulting in a composition of aminium bisulfate ion pair. Meanwhile, a slightly weaker hydrogen bond is formed as well between the adjacent oxygen atom of the sulfuric acid moiety and the hydrogen atom of the amino group, where the O−H distance is 1.740 Å. Apparently, the dual hydrogen bond structure can further stabilize the sulfuric acid−amine complex, in comparison with the single H-bond structure. In this case, the more symmetrical this ring structure, the less tension of the ring, and thereby the more stable the complex. Thus, the lengths of the dual hydrogen bonds are listed in Table 1, as well as their differences ΔR. Interestingly, the ΔR values show a generally consistent trend with the base strength of these primary amines. With the increase of the base strength, ΔR gradually decreases from 0.103 Å of SA-EA to 0.060 Å of SA-IPA. However, an exception exists for SA-tBA, where ΔR equals 0.075 Å and is larger than that of SA-IPA although the base strength of tBA is stronger.

Table 1. Intermolecular O···H Distances of the Dual Hydrogen Bond Structure of Sulfuric Acid-Amine Complexes, Together with their Differences, Calculated at the B3LYP-D3(BJ)/6−311++(3df,3pd) Level of Theory

complex		R_1(O1−H1) (Å)	R_2(O2−H2) (Å)	ΔR (Å)
primary amine-acid	SA-EA	1.637	1.740	0.103
primary amine-acid	SA-PPA	1.651	1.728	0.077
primary amine-acid	SA-IPA	1.666	1.726	0.060
primary amine-acid	SA-tBA	1.667	1.742	0.075
secondary amine-acid	SA-DMA	1.657	1.705	0.048
secondary amine-acid	SA-EMA	1.681	1.725	0.044
tertiary amine-acid	SA-TMA	1.477		

In the secondary amine-sulfuric acid complexes (Figure 2e,f), similar double hydrogen bonds are formed for SA-DMA and SA-EMA. As indicated in Table 1, the ΔR values between two hydrogen bonds are 0.048 Å for SA-DMA and 0.044 Å for SA-EMA, respectively. It is worth noting that the ΔR data in the secondary amine−sulfuric acid complexes are smaller than those of the primary amine−sulfuric acid clusters. In other words, the ring structures of dual hydrogen bonds in secondary amine−sulfuric acid complexes are more symmetrical, indicative of their more stable properties. Moreover, EMA has a slightly smaller ΔR than DMA in acid−amine complexes, which is also consistent with the sequence of their base strength (EMA > DMA). This conclusion provides referential clues for correlation between the structures of the acid−amine complexes with their base strength.

Unlike the above primary and secondary amines, no ring structure can be formed with the interactions between sulfuric acid and the tertiary amine, TMA. As shown in Figure 2g, a sole hydrogen bond is found between sulfuric acid and TMA because of the lack of hydrogen atoms of the amino group. In spite of this, the proton transfer still occurs owing to TMA's role of a strong base. Moreover, the length of O1···H1 is reduced to 1.477 Å as the shortest one among all sulfuric acid−amine complexes, indicative of its strongest hydrogen bonding interaction. In summary, all amine−sulfuric acid complexes in the most stable configuration are identified to be the ion pair form of aminium bisulfate, confirming that ion pairs are preferred to be formed in the nucleation of amines-associated sulfuric acid-driven new particle formation processes.

Based on these optimized geometries, the ZPE-corrected electronic energies (ΔE_{0K}), enthalpies (ΔH_{298K}), and Gibbs free energy changes at 298 K (ΔG_{298K}) of formation were calculated, to assess the enhancing effect on complex stability by different amines in the sulfuric acid-mediated nucleation processes. As listed in Table 2, all ΔG_{298K} values are invariably negative, confirming that the formation of the sulfuric acid−amine complex is thermodynamically favorable. For the primary amine−acid complexes, ΔG_{298K} shows a decreasing order along EA, PPA, IPA, and tBA, which is just opposite to their base strengths. A similar trend is found for the secondary amine-sulfuric acid complexes, SA-EMA is more stable than SA-DMA, as suggested by ΔG_{298K}(SA-EMA) < ΔG_{298K}(SA-DMA). However, the strongest alkali among these amines, TMA, has a smaller ΔG_{298K} absolute value (12.11 kcal·mol^{-1} in Table 2) than EMA for the corresponding formation of acid−amine complexes, at the CCSD(T)/def2-TZVP level. This implies that the base strength is not the unique decisive factor in the enhancing effect of amines on sulfuric acid-containing aerosol particle nucleation.

Generally, the gas-phase basicity of amine is susceptible to substituents owing to inductive effects. The longer and more branched the alkane substituent, the more alkaline the amine. Apparently, the enhanced basicity could promote the formation of aminium bisulfate ion pair by proton transfer

Table 2. ZPE-Corrected Electronic Energies, Enthalpies, and Gibbs Free Energy Changes for the Formation of Sulfuric Acid−Amine Complexes at 298.15 K, where the Optimized Geometries, Harmonic Vibrational Frequencies, and Electronic Energies Were Calculated at both B3LYP-D3(BJ)/6−311++(3df,3pd) and CCSD(T)/def2-TZVP Levels of Theory

complex		ΔE_{0K} (kcal·mol^{-1})		ΔH_{298K} (kcal·mol^{-1})		ΔG_{298K} (kcal·mol^{-1})	
		CCSD(T)	B3LYP	CCSD(T)	B3LYP	CCSD(T)	B3LYP
primary amine-acid	SA-EA	−18.63	−21.06	−18.68	−21.12	−8.21	−10.65
primary amine-acid	SA-PPA	−18.95	−21.44	−18.97	−21.77	−8.38	−11.01
primary amine-acid	SA-IPA	−18.97	−21.78	−18.92	−21.72	−8.53	−11.33
primary amine-acid	SA-tBA	−19.93	−23.01	−19.85	−22.93	−9.30	−12.37
secondary amine-acid	SA-DMA	−20.94	−23.23	−20.83	−23.12	−11.26	−13.54
secondary amine-acid	SA-EMA	−23.07	−25.62	−22.93	−25.48	−12.46	−15.00
tertiary amine-acid	SA-TMA	−22.09	−23.96	−21.85	−23.82	−12.11	−13.98

https://dx.doi.org/10.1021/acs.jpca.0c07908
J. Phys. Chem. A 2020, 124, 10246−10257

from sulfuric acid to amine. To visibly correlate amine basicity with its enhancing effect on sulfuric acid−amine complex stability, the corresponding ΔG_{298K} is plotted versus the gas-phase basicity of the amine as shown in Figure 3. Basically, the

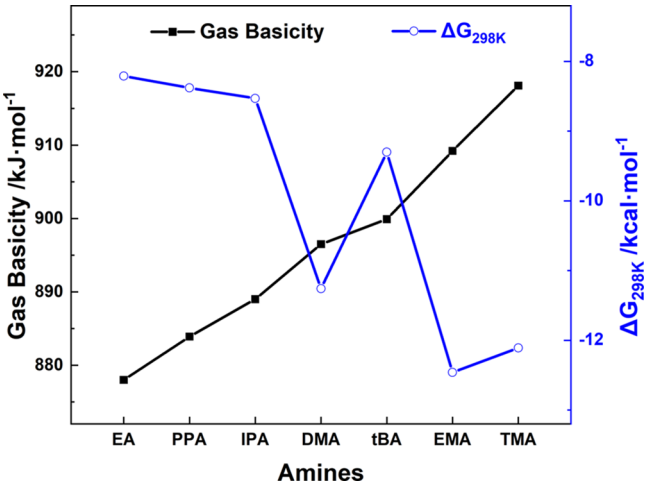

Figure 3. Correlation of gas-phase basicity of amine with Gibbs free energy changes (at the CCSD(T)/def2-TZVP level) for the formation of the corresponding sulfuric acid−amine complex.

primary amine−sulfuric acid complexes follow this deducted rule, as well as the secondary amine-acid clusters. However, ΔG_{298K} of SA-DMA (−11.26 kcal·mol^{-1}) is more negative than that of SA-tBA (ΔG_{298K} = −9.30 kcal·mol^{-1}) at the CCSD(T)/def2-TZVP level, indicating that the nucleation reaction of sulfuric acid and DMA is considerably more effective, although DMA has weaker gas-phase basicity than tBA. Moreover, the strongest alkali among these amines, TMA, also exhibits the weaker stabilizing ability to react with sulfuric acid as indicated by its ΔG_{298K} (−12.11 kcal·mol^{-1}) than the secondary amine, EMA. These two contradictory statements remind us to reexamine the previous conclusion about influence of amine base strength on the stability of sulfuric acid−amine clustering processes.

3.3. Intermolecular Interaction Analyses from QTAIM and NCI Indexes. To understand the intermolecular interaction between sulfuric acid and the amine in depth, QTAIM and NCI indexes were performed specially for hydrogen bonds in the optimized geometries of complexes. Figure 4 shows the calculated bond critical points (BCPs, with orange balls), ring critical points (RCPs, with yellow balls), bond paths (with golden lines), and the NCI isosurfaces within a low reduced density gradient (RDG) range (−0.035∼0.02) for the primary amine−sulfuric acid complexes. Explicit NCIs are manifested in real space with consecutive color-filled regions near BCPs. In addition, RDG versus electron density multiplied by the sign of the second Hessian eigenvalue are plotted in the inserted panels of Figure 4 as well. With the same color scale as the NCI isosurfaces, the blue and green regions indicate attractive and van der Waals interactions, respectively, while the red one implies nonbonding interaction or steric repulsion.

As shown in Figure 4, two BCPs and one RCP along two intermolecular O···H−N bonds were distinctly found for these complexes, confirming the formation of the ring structure. Take the SA-EA complex for instance, two blue isosurfaces located at two BCPs clearly show strong hydrogen bonding interaction between acid and amine, while one red isosurface at RCP indicates steric repulsion of the ring. Interestingly, besides these disk-like isosurfaces, there is a green-brown camber-shaped isosurface between the other free hydroxyl of sulfuric acid and the β-methyl group of amine, indicative of van der Waals interactions within the O···H−C region.

To further understand the above interactions in the view of electron density distributions, Table 3 summarizes the calculated electron density ρ(r), the eigenvalues of the electron-density Hessian matrix (λ_i), and the Laplacian of electron density $\nabla^2\rho$(r) of the hydrogen bonds in the sulfuric acid−amine complexes.

As indicated in Table 3, the formed hydrogen bond via proton transfer has a larger electron density than the other one for all acid−amine complexes in the dual hydrogen bond configuration. Along the sequence of EA → PPA → IPA → tBA, ρ(O1−H1) decreases monotonically from 0.0575 to 0.0532 e·Å^{-3}, while ρ(O2−H2) generally increases. This reduced difference between the electron densities on dual hydrogen bonds agrees with the more symmetrical ring structure and the enhanced complex stability. Moreover, as listed in Table 3, the sign of the Laplacian of electron density in the all complexes is positive, and the sign of the second eigenvalue λ_2 is negative. Thus, both dual O···H−N interactions between acid and amine are typically bonding yet NCIs.

For the secondary amine−acid complexes, very similar NCI isosurfaces were obtained and are shown in Figure 5. On the NCI isosurfaces of SA-EMA, there are also two BCPs and one RCP along two intermolecular O···H−N bonds, together with one green-brown isosurface in the O···H−C region. However, SA-DMA shows some different NCI indexes. No bonding index on its isosurface is found in the O···H−C region because of the lack of any compatible C−H bonds. In comparison to EMA, both ρ(O1−H1) and ρ(O2−H2) of dual hydrogen bonds in SA-DMA are slightly increased. It is worth noting that their electron density difference, ρ(O1−H1) − ρ(O2−H2), decreases monotonically along the sequence of EA → PPA → IPA → tBA → DMA → EMA, which exactly agrees with their base strengths. This consistency distinctly implies that the dual hydrogen bonding interaction depends on the base strength of amines. Additionally, as shown by the RDG scatter plots in the panels of Figure 4, the positions of two blue spikes can visibly exhibit the electron density discrepancies at BCPs along the dual O···H−N bonding paths. Generally, these differences in the primary amine−acid complexes are larger than the counterparts in the secondary amine-acid ones, which is consistent with their asymmetrical ring structures mentioned above.

A different situation exists for the tertiary amine, TMA, when it interacts with sulfuric acid. There is only one blue isosurface for the SA-TMA complex (Figure 5), according to its single hydrogen bond configuration. However, thanks to the relatively adjacent distance between the free oxygen atoms of sulfuric acid and the α-methyl group of amine, two green isosurfaces at BCPs along O···H−C bond paths are observed simultaneously as shown in Figure 5, indicating that the van der Waals attractions between these groups are considerable.

It is worth noting that the largest electron density (0.0856 e·Å^{-3} in Table 3) is obtained for the single O···H−N hydrogen bond of SA-TMA. This just corresponds to its shortest hydrogen bond length. However, this enhanced single hydrogen bond cannot yet compare with dual hydrogen

https://dx.doi.org/10.1021/acs.jpca.0c07908
J. Phys. Chem. A 2020, 124, 10246−10257

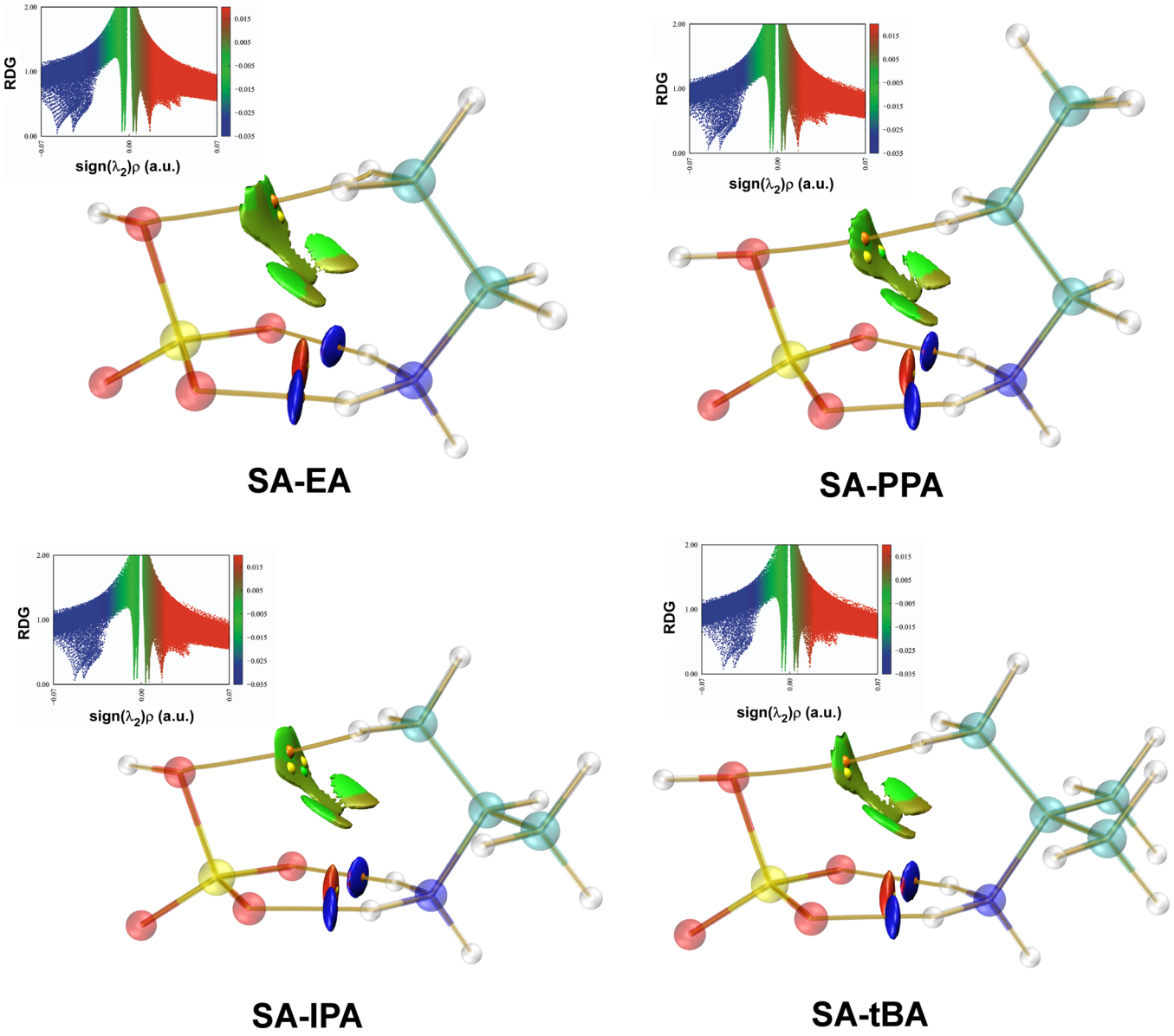

Figure 4. NCI isosurfaces (s = 0.5) of the primary amine−sulfuric acid complexes, where the BCPs and the RCPs are marked with small orange and yellow balls, respectively. RDG versus the electron density multiplied by the sign of the second Hessian eigenvalue is plotted in the inserted panels. All data were obtained by evaluating B3LYP-D3(BJ)/6−311++(3df,3pd) density and gradient values on cuboid grids.

bonding interaction, resulting in its weaker stability than SA-EMA as indicated by ΔG_{298K}. Moreover, in comparison to SA-DMA, two attractions (in green isosurfaces) between the oxygen atom of sulfuric acid and the α-methyl group of amine in SA-TMA provide an extra driving force. This assistance makes the stability of SA-TMA close to that of SA-DMA, as their approximate ΔG_{298K} values in Table 2.

3.4. Enhancing Effect of Amines from the View of Electrostatic Potentials. Although all amine−sulfuric acid complexes have the configuration of aminium bisulfate ion pair formed via proton transfer, the gas-phase basicity of amine does not show a completely consistent trend with its enhancing effect on the complex stability, as indicated in Figure 3. Several exceptions are mentioned above. Therefore, to find the essential correlation between amine properties with the complex stability is crucial for understanding the amine-assisted nucleation mechanism of aerosol particles.

In spite of some minor differences of van der Waals attractions among the seven complexes, the interactions are generally weaker than hydrogen bonding. Thus, we can still attribute the enhancing effect on acid−amine complex stability dominantly to the hydrogen bonding interactions. According to the proton-transfer formation mechanism of aminium bisulfate ion pair, MESP of amines must play a pivotal role therein. Once the first hydrogen bond is formed between sulfuric acid and amine, the attractive interaction between the adjacent oxygen atom of the sulfuric acid moiety and the hydrogen atom of the amino group would naturally promote the formation of the second hydrogen bond, further stabilizing complexes. Therefore, the MESP difference of the nitrogen and hydrogen atoms of amino group, ΔMESP, might be the most significant parameter to determine the ring stability of dual hydrogen bonds. Figure 6 shows the calculated ΔMESP, ΔG_{298K}, and the differences between dual hydrogen bond lengths (ΔR) for all complexes.

https://dx.doi.org/10.1021/acs.jpca.0c07908
J. Phys. Chem. A 2020, 124, 10246−10257

Table 3. Topological Properties at the Hydrogen BCPs in the Sulfuric Acid−Amine Complexes, Calculated at the B3LYP-D3(BJ)/6−311++(3df,3pd) Level

			eigen. of Hessian matrix			
complex	bond	ρ(r) (e·Å^{-3})	λ_1	λ_2	λ_3	$\nabla^2\rho$(r)
SA-EA	O1−H1	0.0575	0.3308	−0.1033	−0.1043	0.1232
	O2−H2	0.0447	0.2667	−0.0719	−0.0710	0.1238
SA-PPA	O1−H1	0.0554	0.3201	−0.0978	−0.0986	0.1237
	O2−H2	0.0460	0.2731	−0.0749	−0.0741	0.1241
SA-IPA	O1−H1	0.0534	0.3111	−0.0930	−0.0936	0.1245
	O2−H2	0.0462	0.2741	−0.0754	−0.0748	0.1239
SA-tBA	O1−H1	0.0532	0.3098	−0.0924	−0.0931	0.1243
	O2−H2	0.0445	0.2660	−0.0715	−0.0707	0.1237
SA-DMA	O1−H1	0.0550	0.3193	−0.0965	−0.0969	0.1259
	O2−H2	0.0489	0.2891	−0.0816	−0.0812	0.1264
SA-EMA	O1−H1	0.0517	0.3027	−0.0884	−0.0888	0.1254
	O2−H2	0.0466	0.2772	−0.0761	−0.0759	0.1252
SA-TMA	O1−H2	0.0856	0.4828	−0.1874	−0.1926	0.1029

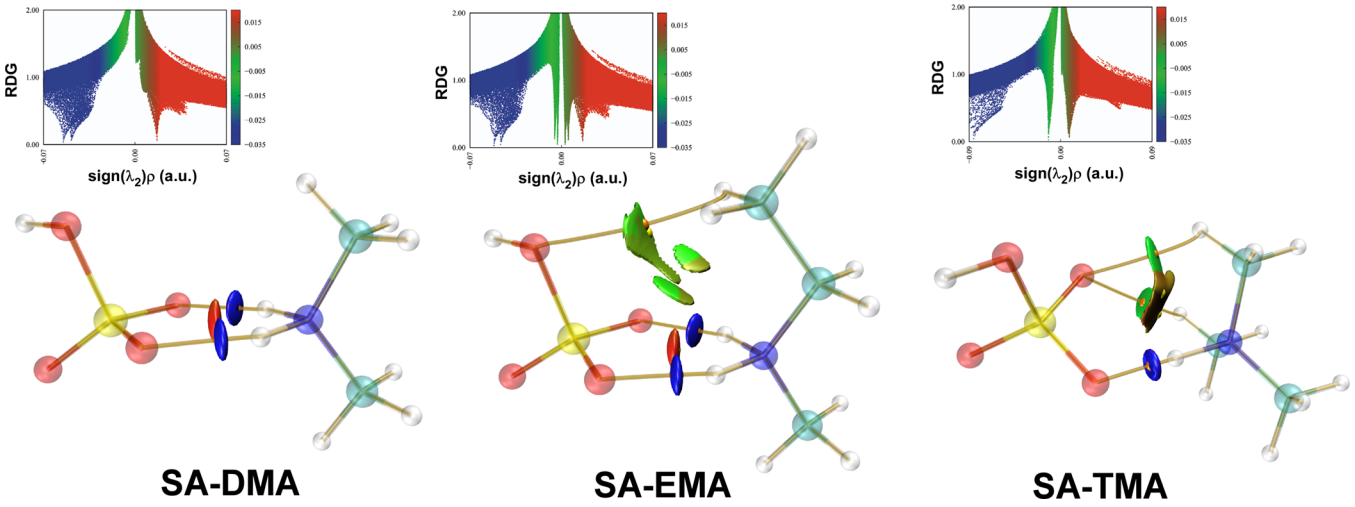

Figure 5. NCI isosurfaces (s = 0.5) of the secondary and tertiary amine−sulfuric acid complexes, where the BCPs and the RCPs are marked with small orange and yellow balls, respectively. RDG versus the electron density multiplied by the sign of the second Hessian eigenvalue is plotted in the inserted panels. All data were obtained by evaluating B3LYP-D3(BJ)/6−311++(3df,3pd) density and gradient values on cuboid grids.

As shown in Figure 6, an approximate consistency is found among ΔMESP, ΔR, Δρ, and ΔG_{298K} for these amines, which is obviously different from their base strength sequence (increase from left to right in Figure 6). This is distinctly inconsistent with the previous conclusions.[41,51] In general, it is comprehensible for amines with a smaller ΔMESP to tend to form more equal dual hydrogen bonds, that is, ΔR of two O···H−N hydrogen bond lengths becomes less with the deceases of ΔMESP and Δρ values. Accordingly, tension of the ring consisting of dual hydrogen bonds in the complexes gradually decreases along this sequence.

However, there are a couple of exceptions among variation tendencies of ΔMESP, ΔR, and ΔG_{298K} as shown in Figure 6. The ΔMESP value of IPA is smaller than that of tBA, however, SA-tBA is less stable than SA-IPA as suggested by their ΔG_{298K}. A similar inconsistency exists for EA and PPA, although their ΔMESP values are very close. Interestingly, all ΔMESP, ΔR, and Δρ data strongly indicate that the ring structure of SA-IPA is slightly more stable than that of SA-tBA, hence, the extra stability effect in the formation of SA-tBA must stem from the other interactions such as van der Waals forces. As mentioned above, van der Waals interactions exist between the free hydroxyl of sulfuric acid and the β-methyl group of amine, regardless of SA-IPA and SA-tBA. As shown in Figure 7, the distances between two interacted moieties in SA-tBA are shorter, while those of SA-IPA are longer, indicative of the stronger attractive interactions in SA-tBA. Actually, this conclusion also can be deduced from the MESP distributions of tBA and IPA. For the IPA monomer, the electrostatic potentials of two hydrogen atoms on β-methyl groups have +9.12 and + 3.76 kcal·mol^{-1}, which are smaller than those in the tBA monomer (+9.60 and + 3.82 kcal·mol^{-1}). Apparently, the higher electrostatic potentials the hydrogen atom has, the stronger the attractive interaction is. Thus, both pieces of evidence indicate van der Waals interactions might be the dominant reason for the reverse sequence of thermodynamic stability for SA-tBA and SA-IPA.

As shown in Table 4, the distance between the free hydroxyl and the β-methyl group of amine in SA-PPA (3.007 Å) is much shorter than that in SA-EA (3.025 Å), which agrees with their electron densities, ρ(SA-PPA) > ρ(SA-EA). Additionally, the positive $\nabla^2\rho$(r) values in Table 4 indicate that this van der Waals interaction plays a role in attractive force. Hence, the stronger van der Waals interaction distinctly exists in SA-PPA

https://dx.doi.org/10.1021/acs.jpca.0c07908
J. Phys. Chem. A 2020, 124, 10246−10257

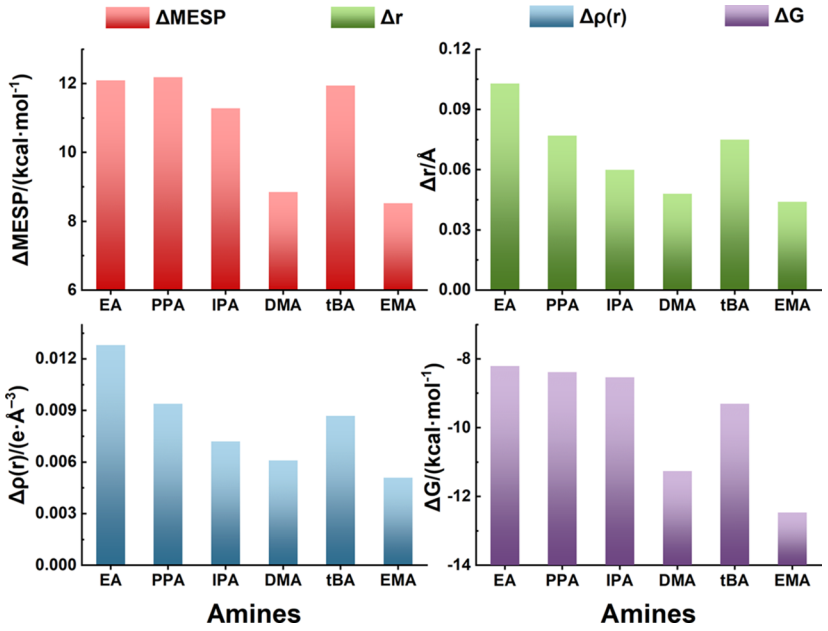

Figure 6. Comparison of the MESP differences of nitrogen and hydrogen atoms of amino group (ΔMESP), the differences between dual hydrogen bond lengths (ΔR), the electron density differences of dual hydrogen bonds (Δρ), and the Gibbs free energy changes for the acid−amine complex formation (ΔG_{298K}). Base strength of the amine increases monotonically from left to right. Data were calculated at the B3LYP-D3(BJ)/6−311++(3df,3pd) level of theory, except that the ΔG_{298K} values were obtained at the CCSD(T)/def2-TZVP level.

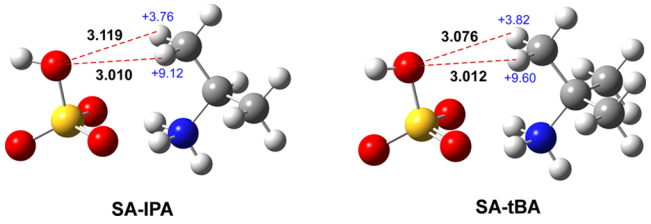

Figure 7. Van der Waals distances (in Å) for SA-IPA and SA-tBA complexes, as well as the MESPs (in kcal·mol^{-1}) for IPA and tBA monomers, calculated at the B3LYP-D3(BJ)/6−311++(3df,3pd) level of theory.

compared with that in SA-EA, which provides an extra assistance for their inverse stabilization energies of SA-EA and SA-PPA.

To summarize, electrostatic potentials on amine surface are central to determine the dual hydrogen bond configuration of the sulfuric acid−amine complexes, and thereby influence the enhancing ability of amine to form sulfuric acid-containing aerosol particles. In other words, the electrostatic potential of amine plays the role of a crucial determinant factor for the thermodynamic stability of sulfuric acid−amine complexes, rather than the basic strength in the gas phase as suggested previously.[41]

3.5. Atmospheric Implication of the Enhancing Effect by Amines on Nucleation. Based on the above structural and thermodynamic analyses, the atmospheric implication of these sulfuric acid−amine complexes can be further illuminated. Since they have similar chemical properties, a direct strategy of assessing their influences is to measure the respective concentrations of sulfuric acid and amines. However, very little experimental data were reported on the concentrations of amines so far, since there are too extensive variations among pristine areas and polluted urban environments. Therefore, the hypothesis of thermodynamic equilibrium is valid for sulfuric acid−amine heterodimer formation, where the intramolecular interactions between sulfuric acid and amine moieties in complexes determine its stability. Consequently, the concentrations of these sulfuric acid−amine complexes can be estimated under atmospheric conditions.

Table 4. Topological Properties at the BCPs along Van der Waals Interactions in the Sulfuric Acid-Amine Complexes, Calculated at the B3LYP-D3(BJ)/6−311++(3df,3pd) Level

			eigen. of Hessian matrix			
complex	distance	ρ(r) (e·Å^{-3})	λ_1	λ_2	λ_3	$\nabla^2\rho$(r)
SA-EA	D(O···H) = 3.025 Å	0.0036	0.0173	−0.0017	−0.0013	0.0143
SA-PPA	D(O···H) = 3.007 Å	0.0037	0.0179	−0.0018	−0.0013	0.0148
SA-IPA	D(O···H) = 3.010 Å, D(O···H) = 3.119 Å	0.0035	0.0169	−0.0015	−0.0008	0.0146
SA-tBA	D(O···H) = 3.012 Å, D(O···H) = 3.076 Å	0.0037	0.0178	−0.0009	−0.0016	0.0153
SA-DMA	−	−	−	−	−	−
SA-EMA	D(O···H) = 3.133 Å	0.0030	0.0144	−0.0011	−0.0006	0.0126
SA-TMA	D(O···H) = 2.381 Å	0.0120	0.0625	−0.0113	−0.0099	0.0413
	D(O···H) = 2.396 Å	0.0121	0.0615	−0.0113	−0.0098	0.0405

https://dx.doi.org/10.1021/acs.jpca.0c07908
J. Phys. Chem. A 2020, 124, 10246−10257

According to the mass-balance relationship, the concentration ratios of sulfuric acid−amine complexes can be expressed in the following eq 1,

$$\frac{[SA{\cdot}A_1]}{[SA{\cdot}A_2]} = \frac{[A_1]}{[A_2]} e^{-\Delta(\Delta G_{298})/RT} \quad (1)$$

where A_1 and A_2 indicate different amines, $\Delta(\Delta G_{298})$ is the difference between the Gibbs free energy of heterodimer formation at 298 K, R is the molar gas constant, and T is the specific temperature, e.g., 298 K in the present study. Assuming that the amine initial concentrations are identical, i.e., $[A_1] = [A_2]$, the concentration ratios of amine-containing complexes relative to that of EA-containing one are vividly shown in Figure 8.

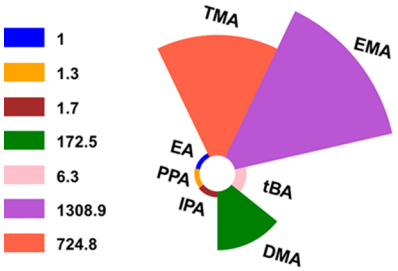

Figure 8. Nightingale rose diagram of the concentration ratios of amine-containing complexes, relative to that of EA-containing one. Data were the corresponding square roots for the purpose of displaying properly.

Along the sequence of EA → PPA → IPA → tBA → DMA → TMA → EMA, the Gibbs free energies of acid−amine complex formation in Table 2 gradually decrease, and thus their concentrations increase exponentially. As shown in Figure 8, in contrast to SA-EA, the concentration of SA-EMA is enhanced ca. 1300-fold owing to its more negative ΔG_{298} by 4.25 kcal·mol^{-1}. In other words, even if the gas-phase EMA concentration is several orders of magnitude lower than that of EA, the corresponding formation of SA-EMA will still be dominant in initial nucleation of atmospheric aerosol particles. However, since this work does not contain nucleation simulations or experiments, it should be stated that the thermodynamic stability of an acid−base complex is not a direct proxy for the nucleation rate under atmospheric conditions. This implies that although ΔG_{298} values can be used to roughly estimate the relative concentrations of these heterodimers, the atmospheric concentration of aerosol particles formed from sulfuric acid−amine reactions might not follow the same order.[50,58,82]

In addition, the absolute concentration of amine could be extremely low in some circumstances, thus, the formation of the sulfuric acid−amine complex will quickly deplete the amine reservoir. Under this action, the thermodynamic equilibrium hypothesis is inappropriate. In addition, the real concentrations of these amines in the atmosphere remain almost unclear yet, and thereby the diagram shown in Figure 8 can only be regarded as a qualitative evaluation of their atmospheric implications. A quantitatively reliable conclusion of amine significance for the corresponding formation of sulfuric acid-containing particles requires integrated investigation on the magnitude and geographical distribution of concentration, which lies beyond the present study scope.

4. CONCLUSIONS

The enhancing effect of seven alkylamines on the thermodynamic stability of sulfuric acid−amine complexes has been theoretically studied here, including EA, PPA, IPA, tBA, DMA, EMA, and TMA. The most stable isomer of the primary and secondary amine-mediated complexes was verified as the pattern of aminium bisulfate ion pairs with a dual hydrogen bond structure, while that of SA-TMA was suggested in the single hydrogen bond configuration because of the lack of hydrogen atoms in the amino group.

Using the optimized geometries, the electrostatic potential analyses of amines truly predicted the acid−amine interaction strengths, which exactly agrees with the amine base strength sequence. This provides a clear illumination for the previously observed correlation between base strength and enhancing effect on complex stability. However, the alkaline sequence of amines is in disagreement with the stabilization energy of the complexes, strongly indicating that the previous conclusion of alkalinity-mediated correlation is not completely correct.

To our surprise, as the core of the acid−amine reaction, ΔMESP of the amino nitrogen atom exhibits the generally consistent trend with the Gibbs free energy changes of formation, ΔG_{298}, of the corresponding sulfuric acid−amine complexes. The QTAIM and NCI index analyses further confirm that the electron density and the dual hydrogen bonding interaction can also correlate with ΔMESP, indicating that this ΔMESP is the true determinant factor for the thermodynamic stability of the complex. Moreover, besides the hydrogen bonding interaction, van der Waals interactions are considerable between the free hydroxyl of sulfuric acid and the β-methyl group of amine and provide an extra stabilizing force in the complexes, especially for sulfuric acid−DMA and sulfuric acid−EMA complexes. Therefore, our conclusions provide new insight into a strategy to assess the enhancing abilities of amines in the sulfuric acid-associated aerosol particle nucleation.

■ ASSOCIATED CONTENT

Supporting Information

The Supporting Information is available free of charge at https://pubs.acs.org/doi/10.1021/acs.jpca.0c07908.

Optimized geometries of sulfuric acid−amine complexes, calculated at the B3LYP-D3(BJ) / 6−311++(3df,3pd) level of theory; optimized geometries of sulfuric acid−amine complexes, calculated at the M06-2X-D3 / 6−311++(3df,3pd) and ωB97XD / 6−311++(3df,3pd) level of theory; gas-phase basicities and proton affinities of amines; and ZPE-corrected electronic energies, enthalpies, and Gibbs free energy changes for the formation of sulfuric acid−amine complexes at 298.15 K calculated at the M06-2X-D3/ 6−311++(3df,3pd) and ωB97XD/6−311++(3df,3pd) level of theory (PDF)

■ AUTHOR INFORMATION

Corresponding Authors

Xiaoguo Zhou − *Hefei National Laboratory for Physical Sciences at the Microscale, Department of Chemical Physics, University of Science and Technology of China, Hefei, Anhui 230026, P. R. China;* orcid.org/0000-0002-0264-0146; Email: xzhou@ustc.edu.cn

https://dx.doi.org/10.1021/acs.jpca.0c07908
J. Phys. Chem. A 2020, 124, 10246−10257

Shilin Liu − *Hefei National Laboratory for Physical Sciences at the Microscale, Department of Chemical Physics, University of Science and Technology of China, Hefei, Anhui 230026, P. R. China*; Email: slliu@ustc.edu.cn

Authors

Jia Han − *Hefei National Laboratory for Physical Sciences at the Microscale, Department of Chemical Physics, University of Science and Technology of China, Hefei, Anhui 230026, P. R. China*

Lei Wang − *Hefei National Laboratory for Physical Sciences at the Microscale, Department of Chemical Physics, University of Science and Technology of China, Hefei, Anhui 230026, P. R. China*

Hanhui Zhang − *Hefei National Laboratory for Physical Sciences at the Microscale, Department of Chemical Physics, University of Science and Technology of China, Hefei, Anhui 230026, P. R. China*

Quyan Su − *Hefei National Laboratory for Physical Sciences at the Microscale, Department of Chemical Physics, University of Science and Technology of China, Hefei, Anhui 230026, P. R. China*

Complete contact information is available at: https://pubs.acs.org/10.1021/acs.jpca.0c07908

Notes

The authors declare no competing financial interest.

■ ACKNOWLEDGMENTS

This work was financially supported by the National Key Research and Development Program of China (No. 2016YFF0200502), the Ministry of Science and Technology of China (No. 2012YQ220113), and the National Natural Science Foundation of China (No. 21873089). The quantum chemical calculations were performed on the supercomputing system in the Supercomputing Center of the University of Science and Technology of China.

■ REFERENCES

(1) Poschl, U. Atmospheric Aerosols: Composition, Transformation, Climate and Health effects. *Angew. Chem., Int. Ed.* **2005**, *44*, 7520−7540.

(2) Charlson, R. J.; Schwartz, S. E.; Hales, J. M.; Cess, R. D.; Coakley, J. A.; Hansen, J. E.; Hofmann, D. J. Climate Forcing by Anthropogenic Aerosols. *Science* **1992**, *255*, 423−430.

(3) Akimoto, H. Global Air Quality and Pollution. *Science* **2003**, *302*, 1716−1719.

(4) Tao, W.-K.; Chen, J.-P.; Li, Z.; Wang, C.; Zhang, C. Impact of Aerosols on Convective Clouds and Precipitation. *Rev. Geophys.* **2012**, *50*, 62.

(5) Lighty, J. S.; Veranth, J. M.; Sarofim, A. F. Combustion Aerosols: Factors Governing Their Size and Composition and Implications to Human Health. *J. Air Waste Manage. Assoc.* **2000**, *50*, 1565−1618.

(6) Lohmann, U.; Feichter, J. Global Indirect Aerosol Effects: A Review. *Atmos. Chem. Phys.* **2005**, *5*, 715−737.

(7) Kulmala, M.; Kontkanen, J.; Junninen, H.; Lehtipalo, K.; Manninen, H. E.; Nieminen, T.; Petaja, T.; Sipila, M.; Schobesberger, S.; Rantala, P.; et al. Direct Observations of Atmospheric Aerosol Nucleation. *Science* **2013**, *339*, 943−946.

(8) Kulmala, M.; Vehkamäki, H.; Petäjä, T.; Dal Maso, M.; Lauri, A.; Kerminen, V.-M.; Birmili, W.; McMurry, P. H. Formation and Growth Rates of Ultrafine Atmospheric Particles: A Review of Observations. *J. Aerosol Sci.* **2004**, *35*, 143−176.

(9) Zhang, R.; Khalizov, A.; Wang, L.; Hu, M.; Xu, W. Nucleation and Growth of Nanoparticles in the Atmosphere. *Chem. Rev.* **2012**, *112*, 1957−2011.

(10) Kulmala, M.; Dal Maso, M.; Mäkelä, J. M.; Pirjola, L.; Väkevä, M.; Aalto, P.; Miikkulainen, P.; Hameri, K.; O'Dowd, C. D. On the Formation, Growth and Composition of Nucleation Mode Particles. *Tellus Ser. B Chem. Phys. Meteorol.* **2001**, *53*, 479−490.

(11) Merikanto, J.; Spracklen, D. V.; Mann, G. W.; Pickering, S. J.; Carslaw, K. S. Impact of Nucleation on Global CCN. *Atmos. Chem. Phys.* **2009**, *9*, 8601−8616.

(12) Zhang, R. Y. Getting to the Critical Nucleus of Aerosol Formation. *Science* **2010**, *328*, 1366−1367.

(13) Sihto, S.-L.; Kulmala, M.; Kerminen, V.-M.; Dal Maso, M.; Petäjä, T.; Riipinen, I.; Korhonen, H.; Arnold, F.; Janson, R.; Boy, M.; et al. Atmospheric Sulphuric Acid and Aerosol Formation: Implications from Atmospheric Measurements for Nucleation and Early Growth Mechanisms. *Atmos. Chem. Phys.* **2006**, *6*, 4079−4091.

(14) Sipila, M.; Berndt, T.; Petaja, T.; Brus, D.; Vanhanen, J.; Stratmann, F.; Patokoski, J.; Mauldin, R. L.; Hyvarinen, A. P.; Lihavainen, H.; et al. The Role of Sulfuric Acid in Atmospheric Nucleation. *Science* **2010**, *327*, 1243−1246.

(15) Weber, R. J.; Marti, J. J.; McMurry, P. H.; Eisele, F. L.; Tanner, D. J.; Jefferson, A. Measured Atmospheric New Particle Formation Rates: Implications for Nucleation Mechanisms. *Chem. Eng. Commun.* **1996**, *151*, 53−64.

(16) Berndt, T.; Böge, O.; Stratmann, F.; Heintzenberg, J.; Kulmala, M. Rapid Formation of Sulfuric Acid Particles at Near-Atmospheric Conditions. *Science* **2005**, *307*, 698.

(17) Young, L.-H.; Benson, D. R.; Kameel, F. R.; Lee, S.-H. Laboratory Studies of H_2SO_4/H_2O Binary Homogeneous Nucleation from the SO_2+OH Reaction: Evaluation of the Experimental Setup and Preliminary Results. *Atmos. Chem. Phys.* **2008**, *8*, 6903−6947.

(18) Ayers, G. P.; Gillett, R. W.; Gras, J. L. On the Vapor Pressure of Sulfuric Acid. *Geophys. Res. Lett.* **1980**, *7*, 433−436.

(19) Marti, J. J.; Jefferson, A.; Cai, X. P.; Richert, C.; McMurry, P. H.; Eisele, F. H_2SO_4 Vapor Pressure of Sulfuric Acid and Ammonium Sulfate Solutions. *J. Geophys. Res. Atmos.* **1997**, *102*, 3725−3735.

(20) Weber, R. J.; McMurry, P. H.; Mauldin, R. L., III; Tanner, D. J.; Eisele, F. L.; Clarke, A. D.; Kapustin, V. N. New Particle Formation in the Remote Troposphere: A Comparison of Observations at Various Sites. *Geophys. Res. Lett.* **1999**, *26*, 307−310.

(21) Nieminen, T.; Manninen, H. E.; Sihto, S.-L.; Yli-Juuti, T.; Mauldin, R. L., III; Petäjä, T.; Riipinen, I.; Kerminen, V.-M.; Kulmala, M. Connection of Sulfuric Acid to Atmospheric Nucleation in Boreal Forest. *Environ. Sci. Technol.* **2009**, *43*, 4715−4721.

(22) Kirkby, J.; Curtius, J.; Almeida, J.; Dunne, E.; Duplissy, J.; Ehrhart, S.; Franchin, A.; Gagne, S.; Ickes, L.; Kurten, A.; et al. Role of Sulphuric Acid, Ammonia and Galactic Cosmic Rays in Atmospheric Aerosol Nucleation. *Nature* **2011**, *476*, 429−433.

(23) Yu, F. Effect of Ammonia on New Particle Formation: A Kinetic H_2SO_4-H_2O-NH_3 Nucleation Model Constrained by Laboratory Measurements. *J. Geophys. Res. Atmos.* **2006**, *111*, D01204.

(24) Kurtén, T.; Torpo, L.; Ding, C.-G.; Vehkamäki, H.; Sundberg, M. R.; Laasonen, K.; Kulmala, M. A Density Functional Study on Water-Sulfuric Acid-Ammonia Clusters and Implications for Atmospheric Cluster Formation. *J. Geophys. Res. Atmos.* **2007**, *112*, D04210.

(25) Almeida, J.; Schobesberger, S.; Kürten, A.; Ortega, I. K.; Kupiainen-Määttä, O.; Praplan, A. P.; Adamov, A.; Amorim, A.; Bianchi, F.; Breitenlechner, M.; et al. Molecular Understanding of Sulphuric Acid-Amine Particle Nucleation in the Atmosphere. *Nature* **2013**, *502*, 359−363.

(26) Paasonen, P.; Olenius, T.; Kupiainen, O.; Kurtén, T.; Petäjä, T.; Birmili, W.; Hamed, A.; Hu, M.; Huey, L. G.; Plass-Duelmer, C.; et al. On the Formation of Sulphuric Acid-Amine Clusters in Varying Atmospheric Conditions and Its Influence on Atmospheric New Particle Formation. *Atmos. Chem. Phys.* **2012**, *12*, 9113−9133.

(27) Yao, L.; Garmash, O.; Bianchi, F.; Zheng, J.; Yan, C.; Kontkanen, J.; Junninen, H.; Mazon, S. B.; Ehn, M.; Paasonen, P.;

et al. Atmospheric New Particle Formation from Sulfuric Acid and Amines in a Chinese Megacity. *Science* **2018**, *361*, 278−281.
(28) Metzger, A.; Verheggen, B.; Dommen, J.; Duplissy, J.; Prevot, A. S. H.; Weingartner, E.; Riipinen, I.; Kulmala, M.; Spracklen, D. V.; Carslaw, K. S.; et al. Evidence for the Role of Organics in Aerosol Particle Formation under Atmospheric Conditions. *Proc. Natl. Acad. Sci. U. S. A.* **2010**, *107*, 6646−6651.
(29) Tröstl, J.; Chuang, W. K.; Gordon, H.; Heinritzi, M.; Yan, C.; Molteni, U.; Ahlm, L.; Frege, C.; Bianchi, F.; Wagner, R.; et al. The Role of Low-Volatility Organic Compounds in Initial Particle Growth in the Atmosphere. *Nature* **2016**, *533*, 527−531.
(30) O'Dowd, C. D.; Jimenez, J. L.; Bahreini, R.; Flagan, R. C.; Seinfeld, J. H.; Hämeri, K.; Pirjola, L.; Kulmala, M.; Jennings, S. G.; Hoffmann, T. Marine Aerosol Formation from Biogenic Iodine Emissions. *Nature* **2002**, *417*, 632−636.
(31) Pechtl, S.; Lovejoy, E. R.; Burkholder, J. B.; Von Glasow, R. Modeling the Possible Role of Iodine Oxides in Atmospheric New Particle Formation. *Atmos. Chem. Phys.* **2006**, *6*, 505−523.
(32) Hou, G. L.; Lin, W.; Deng, S. H. M.; Zhang, J.; Zheng, W. J.; Paesani, F.; Wang, X. B. Negative Ion Photoelectron Spectroscopy Reveals Thermodynamic Advantage of Organic Acids in Facilitating Formation of Bisulfate Ion Clusters: Atmospheric Implications. *J. Phys. Chem. Lett.* **2013**, *4*, 779−785.
(33) Jin, J.; Li, W.; Liu, Y.; Wang, G.; Zhou, M. Infrared Spectroscopic and Theoretical Study of the $HC_{2n+1}O^+$(n=2-5) Cations. *J. Chem. Phys.* **2017**, *146*, 214301.
(34) Li, R. Z.; Zeng, Z.; Hou, G. L.; Xu, H. G.; Zhao, X.; Gao, Y. Q.; Zheng, W. J. Hydration of Potassium Iodide Dimer Studied by Photoelectron Spectroscopy and *ab initio* Calculations. *J. Chem. Phys.* **2016**, *145*, 184307.
(35) Lehtipalo, K.; Yan, C.; Dada, L.; Bianchi, F.; Xiao, M.; Wagner, R.; Stolzenburg, D.; Ahonen, L. R.; Amorim, A.; Baccarini, A.; et al. Multicomponent New Particle Formation from Sulfuric Acid, Ammonia, and Biogenic Vapors. *Sci. Adv.* **2018**, *4*, eaau5363.
(36) Kürten, A.; Bianchi, F.; Almeida, J.; Kupiainen-Määttä, O.; Dunne, E. M.; Duplissy, J.; Williamson, C.; Barmet, P.; Breitenlechner, M.; Dommen, J.; et al. Experimental Particle Formation Rates Spanning Tropospheric Sulfuric Acid and Ammonia Abundances, Ion Production Rates, and Temperatures. *J. Geophys. Res.: Atmos.* **2016**, *121*, 12377−12400.
(37) Torpo, L.; Kurtén, T.; Vehkamäki, H.; Laasonen, K.; Sundberg, M. R.; Kulmala, M. Significance of Ammonia in Growth of Atmospheric Nanoclusters. *J. Phys. Chem. A* **2007**, *111*, 10671−10674.
(38) Weber, R. J.; Marti, J. J.; McMurry, P. H.; Eisele, F. L.; Tanner, D. J.; Jefferson, A. Measurements of New Particle Formation and Ultrafine Particle Growth Rates at a Clean Continental Site. *J. Geophys. Res. Atmos.* **1997**, *102*, 4375−4385.
(39) Jiang, S.; Kong, X.; Wang, C.; Zang, X.; Su, M.; Zheng, H.; Zhang, B.; Li, G.; Xie, H.; Yang, X.; et al. Infrared Spectroscopy of Hydrogen-Bonding Interactions in Neutral Dimethylamine-Methanol Complexes. *J. Phys. Chem. A* **2019**, *123*, 10109−10115.
(40) Angelino, S.; Suess, D. T.; Prather, K. A. Formation of Aerosol Particles from Reactions of Secondary and Tertiary Alkylamines: Characterization by Aerosol Time-of-Flight Mass Spectrometry. *Environ. Sci. Technol.* **2001**, *35*, 3130−3138.
(41) Yu, H.; McGraw, R.; Lee, S.-H. Effects of Amines on Formation of Sub-3 nm Particles and Their Subsequent Growth. *Geophys. Res. Lett.* **2012**, *39*, L02807.
(42) Huang, Y.; Chen, H.; Wang, L.; Yang, X.; Chen, J. Single Particle Analysis of Amines in Ambient Aerosol in Shanghai. *Environ. Chem.* **2012**, *9*, 202−210.
(43) Schobesberger, S.; Franchin, A.; Bianchi, F.; Rondo, L.; Duplissy, J.; Kurten, A.; Ortega, I. K.; Metzger, A.; Schnitzhofer, R.; Almeida, J.; et al. On the Composition of Ammonia-Sulfuric-Acid Ion Clusters during Aerosol Particle Formation. *Atmos. Chem. Phys.* **2015**, *15*, 55−78.
(44) Ge, X.; Wexler, A. S.; Clegg, S. L. Atmospheric Amines−Part I. A Review. *Atmos. Environ.* **2011**, *45*, 524−546.
(45) Barsanti, K. C.; McMurry, P. H.; Smith, J. N. The Potential Contribution of Organic Salts to New Particle Growth. *Atmos. Chem. Phys.* **2009**, *9*, 2949−2957.
(46) Murphy, S. M.; Sorooshian, A.; Kroll, J. H.; Ng, N. L.; Chhabra, P.; Tong, C.; Surratt, J. D.; Knipping, E.; Flagan, R. C.; Seinfeld, J. H. Secondary Aerosol Formation from Atmospheric Reactions of Aliphatic Amines. *Atmos. Chem. Phys.* **2007**, *7*, 289−349.
(47) Bzdek, B. R.; Ridge, D. P.; Johnston, M. V. Amine Exchange into Ammonium Bisulfate and Ammonium Nitrate Nuclei. *Atmos. Chem. Phys.* **2010**, *10*, 3495−3503.
(48) Kurtén, T.; Loukonen, V.; Vehkamäki, H.; Kulmala, M. Amines are Likely to Enhance Neutral and Ion-Induced Sulfuric Acid-Water Nucleation in the Atmosphere More Effectively than Ammonia. *Atmos. Chem. Phys.* **2008**, *8*, 4095−4103.
(49) Nadykto, A.; Yu, F.; Jakovleva, M.; Herb, J.; Xu, Y. Amines in the Earth's Atmosphere: A Density Functional Theory Study of the Thermochemistry of Pre-Nucleation Clusters. *Entropy* **2011**, *13*, 554−569.
(50) Glasoe, W. A.; Volz, K.; Panta, B.; Freshour, N.; Bachman, R.; Hanson, D. R.; McMurry, P. H.; Jen, C. Sulfuric Acid Nucleation: An Experimental Study of the Effect of Seven Bases. *J. Geophys. Res.: Atmos.* **2015**, *120*, 1933−1950.
(51) Myllys, N.; Kubečka, J.; Besel, V.; Alfaouri, D.; Olenius, T.; Smith, J. N.; Passananti, M. Role of Base Strength, Cluster Structure and Charge in Sulfuric-Acid-Driven Particle Formation. *Atmos. Chem. Phys.* **2019**, *19*, 9753−9768.
(52) Kürten, A.; Jokinen, T.; Simon, M.; Sipila, M.; Sarnela, N.; Junninen, H.; Adamov, A.; Almeida, J.; Amorim, A.; Bianchi, F.; et al. Neutral Molecular Cluster Formation of Sulfuric Acid-Dimethylamine Observed in Real Time under Atmospheric Conditions. *Proc. Natl. Acad. Sci. U. S. A.* **2014**, *111*, 15019−15024.
(53) Loukonen, V.; Kurtén, T.; Ortega, I. K.; Vehkamäki, H.; Pádua, A. A. H.; Sellegri, K.; Kulmala, M. Enhancing Effect of Dimethylamine in Sulfuric Acid Nucleation in the Presence of Water - A Computational Study. *Atmos. Chem. Phys.* **2010**, *10*, 4961−4974.
(54) Lv, S. S.; Miao, S. K.; Ma, Y.; Zhang, M. M.; Wen, Y.; Wang, C. Y.; Zhu, Y. P.; Huang, W. Properties and Atmospheric Implication of Methylamine Sulfuric Acid-Water Clusters. *J. Phys. Chem. A* **2015**, *119*, 8657−8666.
(55) Hong, Y.; Liu, Y. R.; Wen, H.; Miao, S. K.; Huang, T.; Peng, X. Q.; Jiang, S.; Feng, Y. J.; Huang, W. Interaction of Oxalic Acid with Methylamine and Its Atmospheric Implications. *RSC Adv.* **2018**, *8*, 7225−7234.
(56) Miao, S. K.; Jiang, S.; Peng, X. Q.; Liu, Y. R.; Feng, Y. J.; Wang, Y. B.; Zhao, F.; Huang, T.; Huang, W. Hydration of the Methanesulfonate-Ammonia/Amine Complex and Its Atmospheric Implications. *RSC Adv.* **2018**, *8*, 3250−3263.
(57) Wang, C. Y.; Jiang, S.; Liu, Y. R.; Wen, H.; Wang, Z. Q.; Han, Y. J.; Huang, T.; Huang, W. Synergistic Effect of Ammonia and Methylamine on Nucleation in the Earth's Atmosphere. A Theoretical Study. *J. Phys. Chem. A* **2018**, *122*, 3470−3479.
(58) Jen, C. N.; McMurry, P. H.; Hanson, D. R. Stabilization of Sulfuric Acid Dimers by Ammonia, Methylamine, Dimethylamine, and Trimethylamine. *J. Geophys. Res.: Atmos.* **2014**, *119*, 7502−7514.
(59) Hunter, E. P. L.; Lias, S. G. Evaluated Gas Phase Basicities and Proton Affinities of Molecules: An Update. *J. Phys. Chem. Ref. Data* **1998**, *27*, 413−656.
(60) Lu, T. *Molclus program, Version 1.9.3.* http://www.keinsci.com/research/molclus.html (accessed May 7, 2020).
(61) Korth, M. Third-Generation Hydrogen-Bonding Corrections for Semiempirical QM Methods and Force Fields. *J. Chem. Theory Comput.* **2010**, *6*, 3808−3816.
(62) Stewart, J. J. P. *MOPAC2016*, Stewart Computational Chemistry, Colorado Springs, CO, USA,: 2016.
(63) Neese, F. The ORCA program system. *WIREs Comput. Mol. Sci.* **2012**, *2*, 73−78.
(64) Neese, F. Software Update: the ORCA Program System, Version 4.0. *WIREs Comput. Mol. Sci.* **2018**, *8*, e1327.

https://dx.doi.org/10.1021/acs.jpca.0c07908
J. Phys. Chem. A 2020, 124, 10246−10257

(65) Brandenburg, J. G.; Bannwarth, C.; Hansen, A.; Grimme, S. B97-3c: A Revised Low-Cost Variant of the B97-D Density Functional Method. *J. Chem. Phys.* **2018**, *148*, No. 064104.
(66) Frisch, M. J.; Trucks, G. W.; Schlegel, H. B.; Scuseria, G. E.; Robb, M. A.; Cheeseman, J. R.; Scalmani, G.; Barone, V.; Petersson, G. A.; Nakatsuji, H., et al. *Gaussian 16, Revision C.01*; Gaussian, Inc.: Wallingford, CT, 2016.
(67) Grimme, S.; Ehrlich, S.; Goerigk, L. Effect of the Damping Function in Dispersion Corrected Density Functional Theory. *J. Comput. Chem.* **2011**, *32*, 1456−1465.
(68) Emamian, S.; Lu, T.; Kruse, H.; Emamian, H. Exploring Nature and Predicting Strength of Hydrogen Bonds: A Correlation Analysis Between Atoms-in-Molecules Descriptors, Binding Energies, and Energy Components of Symmetry-Adapted Perturbation Theory. *J. Comput. Chem.* **2019**, *40*, 2868−2881.
(69) Raghavachari, K.; Trucks, G. W.; Pople, J. A.; Head-Gordon, M. A Fifth-Order Perturbation Comparison of Electron Correlation Theories. *Chem. Phys. Lett.* **1989**, *157*, 479−483.
(70) Myllys, N.; Elm, J.; Halonen, R.; Kurtén, T.; Vehkamäki, H. Coupled Cluster Evaluation of the Stability of Atmospheric Acid-Base Clusters with up to 10 Molecules. *J. Phys. Chem. A* **2016**, *120*, 621−630.
(71) Weigend, F.; Ahlrichs, R. Balanced Basis Sets of Split Valence, Triple Zeta Valence and Quadruple Zeta Valence Quality for H to Rn: Design and Assessment of Accuracy. *Phys. Chem. Chem. Phys.* **2005**, *7*, 3297−3305.
(72) Bader, R. F. W.; Nguyen-Dang, T. T.; Tal, Y. A Topological Theory of Molecular Structure. *Rep. Prog. Phys.* **1981**, *44*, 893−948.
(73) Bader, R. F. W.; Essén, H. The Characterization of Atomic Interactions. *J. Chem. Phys.* **1984**, *80*, 1943−1960.
(74) Bader, R. F. W. Atoms In Molecules. *Acc. Chem. Res.* **1985**, *18*, 9−15.
(75) Bader, R. F. W. A Quantum Theory of Molecular Structure and Its Applications. *Chem. Rev.* **1991**, *91*, 893−928.
(76) Bader, R. F. W. Comment on the Comparative Use of the Electron Density and Its Laplacian. *Chem. − Eur. J.* **2006**, *12*, 7769−7772.
(77) Johnson, E. R.; Keinan, S.; Mori-Sánchez, P.; Contreras-García, J.; Cohen, A. J.; Yang, W. Revealing Noncovalent Interactions. *J. Am. Chem. Soc.* **2010**, *132*, 6498−6506.
(78) Lu, T.; Chen, F. Multiwfn: A Multifunctional Wavefunction Analyzer. *J. Comput. Chem.* **2012**, *33*, 580−592.
(79) Murray, P. P. J. S., In *Reviews in Computational Chemistry*, 1991; *2*, 273−312.
(80) Murray, J. S.; Politzer, P. The Electrostatic Potential: An Overview. *WIREs Comput. Mol. Sci.* **2011**, *1*, 153−163.
(81) Murray, J. S.; Politzer, P. Molecular Electrostatic Potentials and Noncovalent Interactions. *WIREs Comput. Mol. Sci.* **2017**, *7*, e1326.
(82) Myllys, N.; Ponkkonen, T.; Chee, S.; Smith, J. Enhancing Potential of Trimethylamine Oxide on Atmospheric Particle Formation. *Atmosphere* **2020**, *11*, 18.

https://dx.doi.org/10.1021/acs.jpca.0c07908
J. Phys. Chem. A 2020, 124, 10246−10257